Available online at www.sciencedirect.com
ScienceDirect
Polymer 48 (2007) 5994–6001
polymer
www.elsevier.com/locate/polymer

Unique morphology and properties study of polyacrylate obtained *via* frontal photopolymerization☆

Yanyan Cui, Jianwen Yang*, Zhaohua Zeng, Zhi Zeng, Yonglie Chen

Institute of Polymer Science, School of Chemistry and Chemical Engineering, Sun Yat-Sen University, Guangzhou 510275, China

Received 8 February 2007; received in revised form 22 July 2007; accepted 3 August 2007
Available online 9 August 2007

Abstract

Remarkable radial temperature distribution at the advancing reaction front was determined in frontal photopolymerization (FPP). Through SEM observation of the cross-fracture section and vertical fracture section for the heat-insulated FPP polymer rod, a cylindrical multi-layer structure was first observed in the FPP product. A sleeve-like model was proposed to describe the unusual morphology on the basis of polymer self-drawing and convection around reaction front. Vertical gradient distribution of molecular weight and its polydispersity in the poly(isobornyl acrylate) rod obtained *via* FPP was found through GPC determination, which might be developed as an *in situ* self-fractionation technique for polymer. Thermal analysis of the polymers showed that the FPP tended to produce purer polymer than the traditional thick film photopolymerization.

Keywords: Frontal polymerization; Photopolymerization; Morphology

1. Introduction

Frontal polymerization (FP) is a reaction mode of converting monomer into polymer via a localized and propagating reaction zone in a tube [1]. By this reaction mode, some functional gradient materials (optic materials) [2], interpenetrating polymer networks [3], hydrogel [4], and a new process for *in situ* reinforcement of porous materials [5] have been developed. In most cases of FP, significant pressure in the tube may be generated due to the acute exothermic polymerization in fronts and may potentially lead to explosion. The high temperature front in FP is a dilemma. It is necessary for accelerating the propagation of polymerization front, but increases the risk of explosion and evaporation of monomers. As a widely used fast synthetic technique, photopolymerization encounters difficulty while applying in thick or bulk materials due to the limited penetration of incident UV light. Fortunately, a photobleaching initiation system permits the effective penetration of incident UV/visible light and makes possible the frontal photopolymerization (FPP) [6–8]. With photopolymerization, the temperature of propagation front may be lowered down to a moderate level so that the defects of large voids, buoyancy-driven convection in the obtained polymer may be avoided or decreased. The studies on the kinetics of FPP were mostly concentrated on mathematical simulations of ideal reaction model. Some useful predictions of spatiotemporal kinetics were obtained [9–11]. Experimental investigations of frontal photopolymerization were focused on the spatiotemporal kinetics including species spatiotemporal distributions and the traveling velocity of polymerization fronts [12–14]. As a primary aspect of frontal photopolymerization, the morphology investigation for the frontal photopolymerization products was necessary due to the potential influence of convection and the Rayleigh–Taylor effect [15,16] during front propagation. In the present research, the morphologies, thermal behaviors and depth-resolved molecular weight of the FPP products were investigated.

☆ Project supported by the National Natural Science Foundation of China (Grant Nos. 20304019 and 60378029).
* Corresponding author.
E-mail address: cesyjw@mail.sysu.edu.cn (J. Yang).

0032-3861/$ - see front matter © 2007 Elsevier Ltd. All rights reserved.
doi:10.1016/j.polymer.2007.08.013

2. Experimental part

2.1. Materials

2,4,6-Trimethylbenzoyldiphenylphosphine oxide (TPO), as a photoinitiator, was obtained from Ciba. Isobornyl acrylate (IBOA), a monomer with lower polymerization shrinkage and high boiling point, was donated by Eternal Chemical Co. Ltd. (Zhuhai, China). All of the chemicals were used without further purification.

2.2. Conduction of FPP

The photoinitiator TPO (2.0 wt %) was dissolved in IBOA and then added to a vertical pipe having an inner diameter of 7 mm and encased with a rubber bulb at the bottom. The soft bulb could compensate for the volume shrinkage which was caused by the conversion of monomer in the upper layer into polymer. With this shrinkage compensation, huge hollows could be eliminated and FPP front could steadily propagate. The filled pipe was fixed vertically in a chamber and covered with a punched black board to make the sample only be irradiated perpendicularly and prevent side irradiation. A 125 W Philips medium pressure mercury lamp, with high efficient UV output and low heat emission, was employed as an UV source. The light intensity on the irradiation surface, which varied with distance from the lamp, was measured with an UVA radiometer of which detector was sensitive to the photon ranging from 320 to 400 nm. The FPP was investigated under three different circumstances, namely salty ice cooling (initial temperature −3 °C), ambient conduction without any control (at r.t. or r.t. FPP) and heat insulation with cotton wrapping. For the insulated FPP, the reaction pipe, tightly packed with cotton on the wall, could be regarded as quasi-adiabatic system during exothermic photopolymerization.

2.3. Temperature profiles

The radial temperature profiles of FPP systems corresponding to the axial center and pipe wall at the same latitude were monitored with two tiny thermocouples which arrayed in the monomer along with the pipe. All of the installed thermocouples were connected with a digital electrometer and the displayed temperature variations with irradiation time were recorded by video camera.

2.4. Polymer characterization

Scanning electron microscopy of the FPP polymer, fractured in liquid nitrogen, was performed with a JEOL JSM-6330F SEM. IR spectra, using KBr pellet, were recorded on a Nicolet Nexus-670 FT-IR spectrometer to determine the conversion of IBOA. Differential scanning calorimeter (DSC) traces were obtained with a TA MDSC 2910 calorimeter at a heating rate of 10 °C/min under nitrogen atmosphere. Netzsch TG-209 thermogravimetric analyzer (TGA) was adopted to compare the FPP polymer with that of a thick film obtained by traditional photopolymerization, in which the samples were dried under vacuum and the heating rate was controlled at 10 °C/min under nitrogen atmosphere. The average molecular weight of polymer was measured by Waters Breeze Gel Permeation Chromatograph (GPC) with polystyrene as standard.

3. Results and discussion

The existence of photopolymerization front was a basic aspect of FPP which was contrasted to simple deep photopolymerization. IR spectroscopy was applied to determine the spatial conversion of monomer in the tube. The obtained polymer rod was cut into small segments at an interval of 5 mm and each segment was subjected to FT-IR measurement. The decreasing absorption band at 810 cm^{-1} with conversion of IBOA was used for calculation of IBOA conversion, using the carbonyl absorption band at 1720 cm^{-1} as an internal standard. The spatial conversions of IBOA under different conditions are plotted in Fig. 1. It was shown that the conversions of IBOA in upper layer under three conditions were complete and dropped suddenly at certain depth, which signified the existence of photopolymerization front.

Great axial (vertical along the tube) temperature gradient had been discussed in traditional thermal FP systems. Due to thermal diffusion and conduction, there must be a radial temperature distribution in the FPP tube, which might be an another important factor to influence the front figuration and morphology of the produced FPP polymer. The radial temperature falls in IBOA FPP system were recorded by measuring the temperature at axial center and closing the tube wall. The plots of temperature *vs* irradiation time at two points (center and wall) are shown in Fig. 2.

With the polymerization front traveling, the temperature detected by thermocouples increased drastically and then tended to decrease after the thermocouples were left behind the front. As shown in Fig. 2a, the temperature difference between the axial center and the tube wall for the ice-cooled one was only around 3 °C even at the peak temperature, which meant that there was no obvious radial temperature gradient in

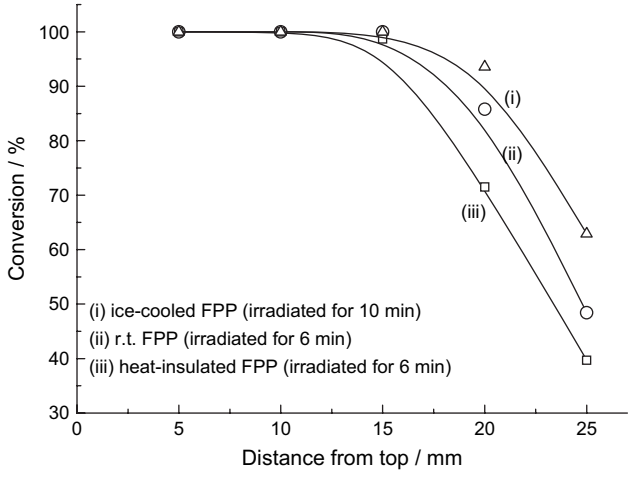

Fig. 1. Spatial conversion of IBOA FPP at different conditions (light intensity: 5.5 mW/cm^2).

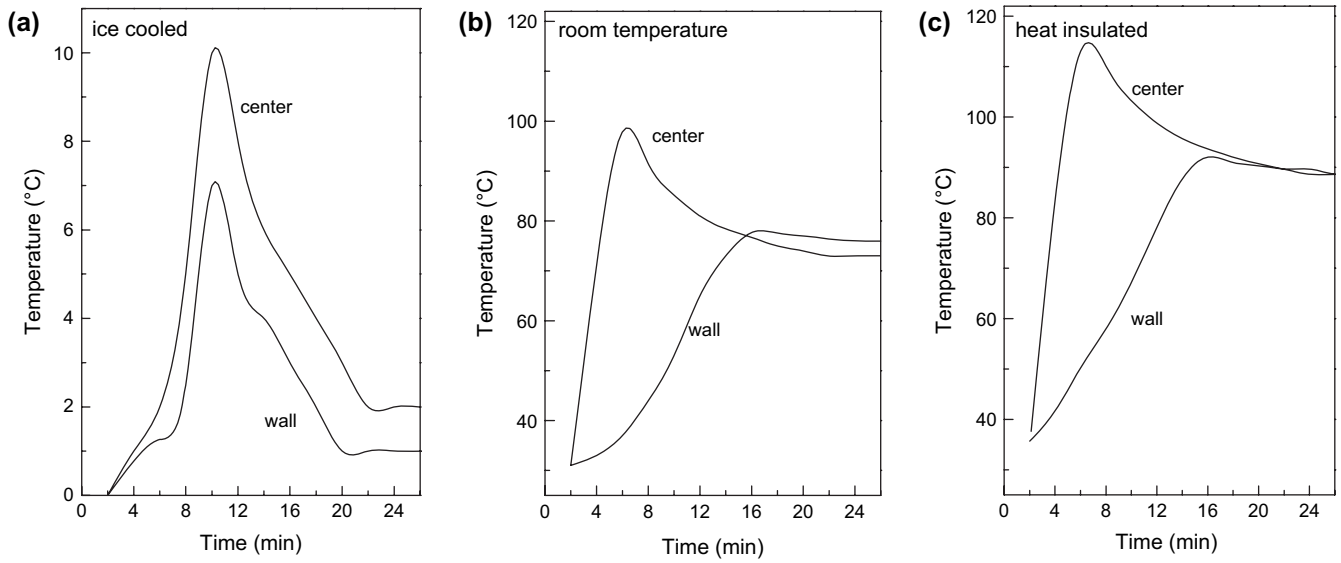

Fig. 2. Radial temperature gradient with irradiation in FPP tube under different conditions (light intensity: 5.5 mW/cm^2; pipe diameter: 7.0 mm).

the ice-cooled run. However, a remarkable radial temperature difference, reaching the maximum of about 60 °C, occurred in the r.t. and heat-insulated FPP systems based on Fig. 2b and c. It was thus possible that a transverse convection and thermal diffusion existed in the latter two FPP systems.

For an ideal FP system, the propagating front was supposed to be a perfect plane. It was also found that the polymerization front of IBOA under ice-cooled circumstance is presented as a perfect plane due to controlled temperature effect (Fig. 3a). However, radial and/or vertical temperature gradient could not be avoided in the heat insulated and r.t. FPP systems due to the exothermic accumulation of polymerization. The reaction front thus advanced ahead accompanied with thermal convection and Rayleigh–Taylor effect within the traveling reaction zone, leading to a bulged front if the FPP process was terminated abruptly and the residual liquid monomer was removed (as shown in Fig. 3b and c). The stalactiform front could be easily understood with the typical Rayleigh–Taylor effect.

As indicated in Fig. 2, the maximum front temperature was close to 100 °C for r.t. FPP of IBOA and reached 114 °C for the heat-insulated run, which is beyond the glass transition temperature of poly(IBOA) (94 °C [17]). The poly(IBOA) formed at early stage in the front zone would be a hot viscous fluid with greater density than the monomer. With the influences of many factors, including the density difference, front temperature increased and descending traveling of front, a great Rayleigh–Taylor effect was thus resulted and responsible for the bulged front.

Except for the bulged front formed in the FPP of IBOA under r.t. and heat-insulated circumstance, the FPP polymers thus obtained were found to exhibit special morphology which was greatly different from that obtained under ice-cooled condition. A uniform morphology was observed for the polymer obtained under ice-cooled condition (Fig. 4). The smooth fracture section could be attributed to the lack of temperature gradient during FPP. The polymer was produced by steady advancing of

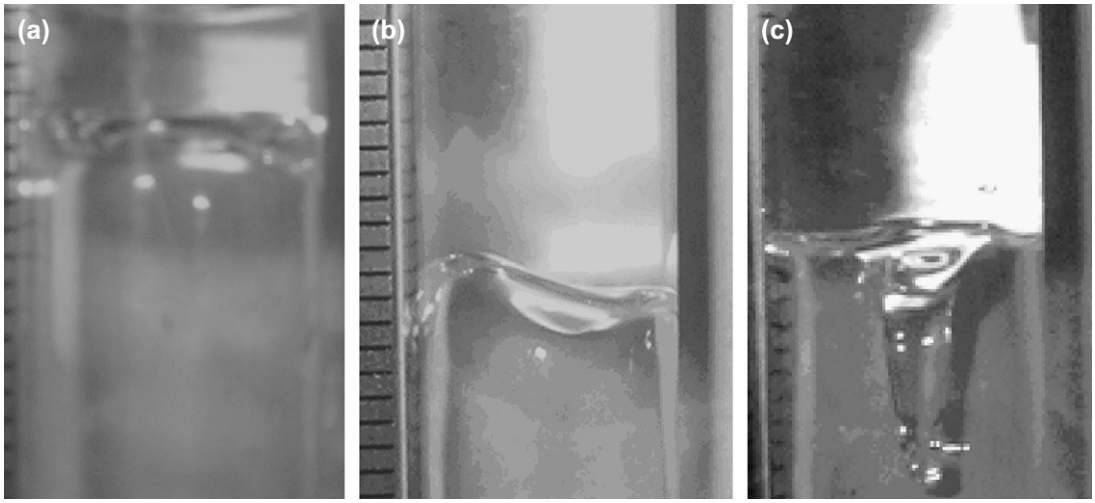

Fig. 3. The bulged front of IBOAFPP under different conditions (a) ice-cooled, (b) r.t. and (c) heat insulated (light intensity: 5.5 mW/cm^2).

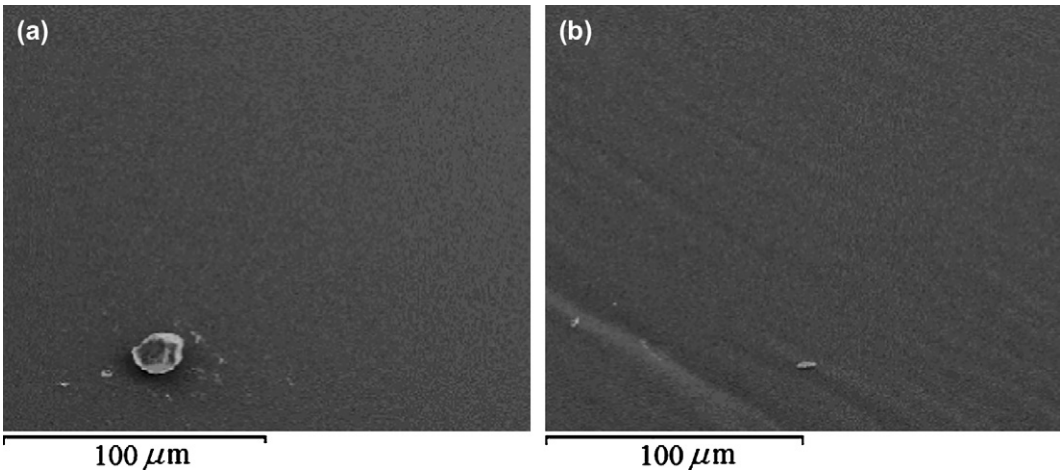

Fig. 4. SEM micrograph of poly(IBOA) obtained via FPP under ice-cooled condition (a) vertical section and (b) cross-section (light intensity: 5.5 mW/cm^2).

front without Rayleigh–Taylor effect and transverse convection. As indicated in Fig. 2a, the front temperature for the ice-cooled FPP of IBOA was much lower than the glass transition temperature of poly(IBOA). The polymer chain propagating

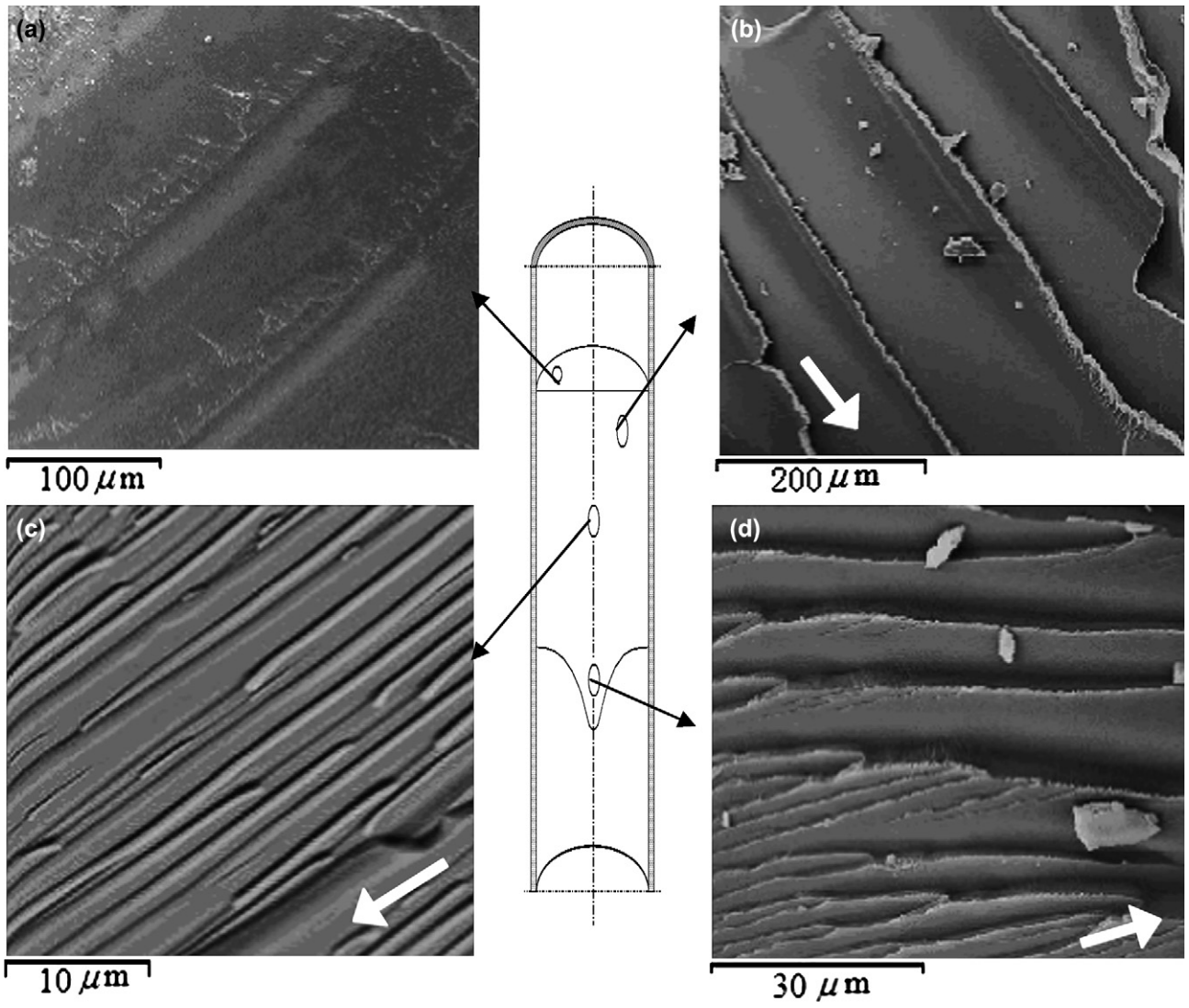

Fig. 5. SEM micrograph of poly(IBOA) obtained via FPP under heat-insulated condition (a) cross-section; (b), (c) and (d) vertical section. (The white arrows in micrographs indicate the traveling direction of polymerization front; light intensity: 5.5 mW/cm^2.)

in the cold front was almost in frozen state except for the initial oligomer stage. The polymer formed and/or forming in the front zone had no chance to sag due to vitrification.

In Fig. 5, circular striations were found for the cross-sections (micrograph a) and multi-layer structure for the vertical section (micrographs b and c). The arc striations in Fig. 5a were considered as ductile fracture, but the interzone bands among the striations were brittle fracture. The multi-layer morphology in Fig. 5b and c, which was the micro-observation of the vertical fracture surface of FPP polymer rod, suggested that the poly-(IBOA) was formed in a multi-layer cylindrical structure along with the polymerization front propagation. The morphology of rut-like striations in Fig. 5a is basically in accordant with that of the stacked cylindric layers of vertical fracture surface in Fig. 5b and c. The difference between Fig. 5b and c could be attributed to the distance of observing surface from the axis. Similar striations and multi-layer morphology were also found on the fracture surface of r.t. FPP polymer rod of IBOA.

The observed result (Fig. 5c) corresponding to the axis vicinity of vertical fracture surface showed fine oriented layers in the thickness of around a few micrometers, even though the single layer was not continuous in appearance. Another interesting morphology corresponding to the vertical section closing to the bulged front is shown in Fig. 5d. In this micrograph, polymer flow tide toward the advancing front was observed. Due to the vertical and radial temperature gradients, and the density difference between polymer and monomer, the influence of Rayleigh–Taylor effect and convection [18] on the micro-topography of obtained polymer could not be ignored.

The aforementioned peculiar micro-topology, circular striations on the cross-section and parallel cylindric layers, might be ascribed to the Rayleigh–Taylor effect and transverse temperature gradient. Because the temperature at the center of bulged front was higher than that at the tube wall and the front drooped at center with FPP undergoing, an axisymmetric circumfluence of monomer and oligomer was proposed for understanding the forming of oriented polymer layers and striations (Fig. 5). The hot and drooping front would drive the vicinal hot monomer to diffuse downward [19], but the buoyancy effect would resist the diffusion and thus the hot flow turned toward the cold boundary. Finally, rounded convection was produced with the suppression of down-traveling front. With the cyclic axisymmetric circumfluence and continuous advancing of the front, polymer was generated wrapping the protruded front layer by layer and formed a sleeve-like structure as illustrated in Fig. 6. The oriented polymer sleeve generally had a wall thickness of a few micrometers and it was suggested that the descending FPP of IBOA at r.t. or under heat insulation might be applied in the assembly and orientation of nano-fiber, nano-tube or nano-rod.

On the other hand, viscoelastic theory [20] could also be applied for understanding the macro-orientation in FPP. As shown in Fig. 2, the temperature at the front center for heat insulated and r.t. FPP was higher than that for ice-cooled FPP. The polymer in the center of hot front zone was in viscoelastic state and could sag because of its fairly greater density than the monomer. The downflow of viscoelastic polymer would

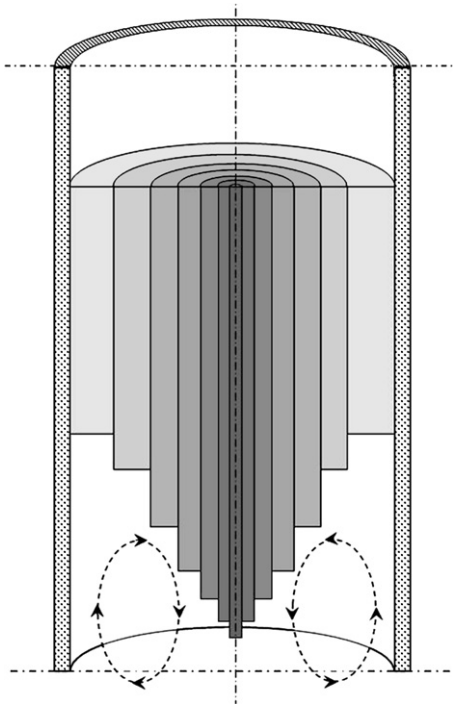

Fig. 6. Sleeve-like descending front with axisymmetric mode of convection.

force the polymer chain segment to orientate partially along with the sagging direction. The XRD patterns of the three FPP samples, gave some clues to the partial orientation of FPP polymer chain (see Fig. s1 in the Supplementary data).

FPP was a fairly new polymerization method. It was very necessary to measure the molecular weight of poly(IBOA). A polymer rod sample obtained *via* r.t FPP was cut into segments at intervals of 8 mm from the top surface and then subjected to GPC analysis with THF as solvent. The depth-resolved number average molecular weight (M_n), weight average molecular weight (M_w) and molecular weight distribution (MWD) are shown in Fig. 7.

According to Pojman and Epstein, no substantial difference in molecular weight of polymers was found between those obtained by thermal frontal polymerization and classic pot polymerization [21]. Moreover, the depth-resolved molecular weight had not been reported in the literatures. The M_w, M_n and MWD of the thick film samples obtained *via* traditional photopolymerization were determined to be 9.12×10^4, 2.16×10^4 and 4.23, respectively. Fig. 7 showed that the FPP products all gave higher molecular weight in contrast to the thick film photopolymerization. Based on the kinetics of bulk polymerization, the monomer concentration decreased steadily with reaction proceeding. However, the frontal reaction zone always kept in contact with the bulk monomer and the monomer concentration in frontal zone could be regarded as a constant except in the heavy gelation stage. Persistent high concentration of monomer was usually favorable for producing polymer with high molecular weight. Of course, the whole kinetics of FPP was complex because the influence of gelation, variation of propagation and termination were not easy to simulate. The more attractive result indicated in Fig. 7 was that the

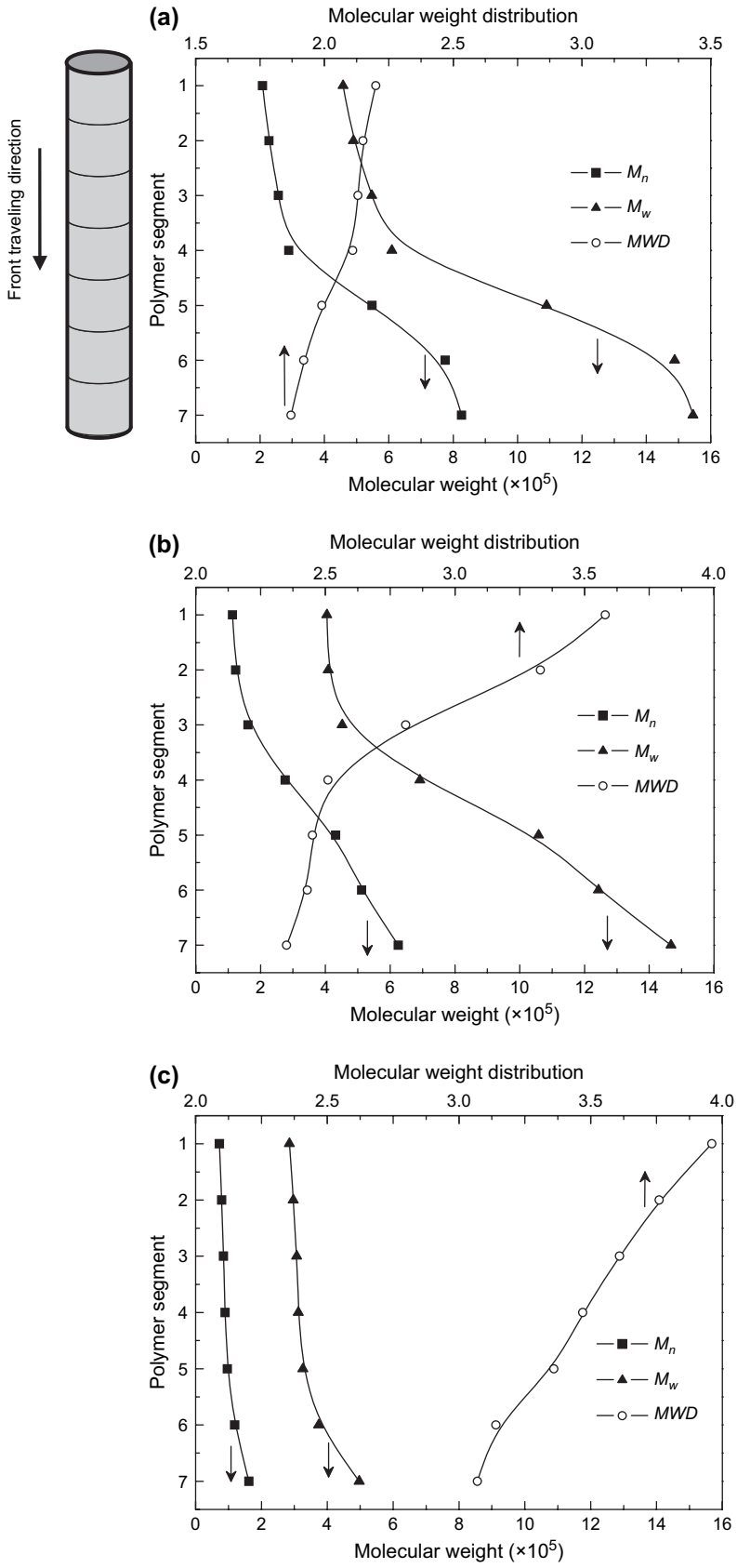

Fig. 7. The depth-resolved molecular weight and molecular weight distribution for the FPP polymer obtained at (a) ice-cooled, (b) r.t. and (c) heat insulated (light intensity: 4.3 mW/cm^2).

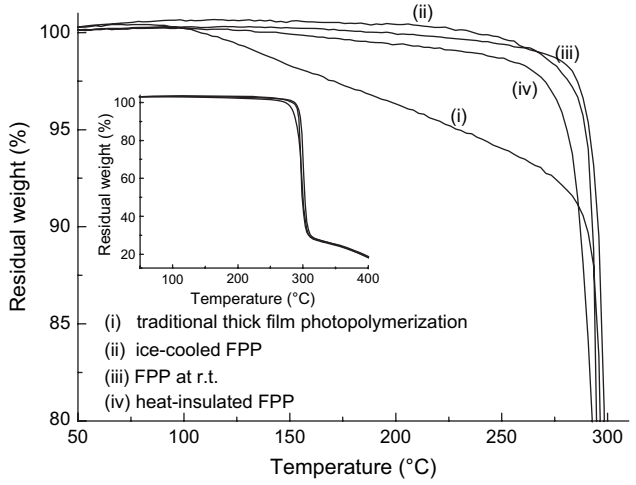

Fig. 8. TGA traces of poly(IBOA) obtained at different conditions (light intensity: 5.5 mW/cm^2).

molecular weight increased with sample depth while the MWD decreased steadily. The vertical gradient distributions of molecular weight and MWD accorded with the attenuation of light intensity in the FPP tube, which was induced by the absorption and reflection of the formed polymer. The gradient distribution was addressed as ''*in situ* self-fractionation'' of polymer. It was well-known that the properties and performance of polymer materials depended on its molecular weight to great extent. Through designing of FPP procedure, one could readily obtain a polymer with certain molecular weight and MWD by cutting out different portions from the polymer rod. Moreover, the gradient polymer from modified FPP technique might be potentially applied as gradient optical material and damping material. But distinct differences were observed for different polymerization conditions.

The influence of FPP circumstance on the molecular weight gradient was also indicated in Fig. 7 (a–c). Higher front temperature for the heat-insulated FPP over the r.t. FPP would decrease the molecular weight and broaden MWD (Fig. 7c) due to the enhanced chain termination. High temperature in polymerization front also decreased the viscosity of early formed polymer and accelerated the convection around the polymerization front. It could be regarded as improved agitation and thus reduced the vertical gradient of molecular weight in FPP polymer rod.

Thermal analysis, TGA and DSC had been conducted to investigate the frontal polymerization products. Nevertheless, it had been reported that there was scarce difference in thermal analysis results between a classic bulk polymerization product and the thermal FP [22]. In present research, four photopolymerization products, including thick film poly(IBOA) obtained via traditional photopolymerization in air (i) [*ca.* 3 mm in thickness, irradiated for 15 min with light intensity of 5.5 mW/cm^2] and poly(IBOA) obtained via FPP under salty ice-cooled (ii), ambient temperature (iii) and heat insulated (iv), were subjected to TGA and DSC measurements. For the FPP polymer rods (ii–iv), the samples at the depth of 16–24 mm were selected for thermal analysis. As shown in Fig. 8, distinct difference was observed for the weight loss traces. Great weight loss was revealed for the thick film photopolymerization product. It might be ascribed to the evaporation of residual monomer enclosed in the solid poly(IBOA). The FPP polymers were found to exhibit good thermal stability of up to 250 °C. It was suggested that residual monomer could be squeezed out from the *in situ* formed polymer during FPP process and pure polymer was facilely produced. The FPP could be taken as a potential technique to *in situ* produced pure polymer in contrast to traditional photopolymerization.

The DSC traces for the four samples (i–iv) are shown in Fig. 9. The first scanning traces shown in Fig. 9a clearly indicated the prominent enthalpy relaxation around the glass transition temperature. It was not strange if considered the thermal history of the samples accumulated during fast polymerization. The irreversible enthalpy which reflected the entanglement of amorphous polymer chain could be measured with the modulated DSC analysis if needed [23]. For the samples of thick film photopolymerization, r.t. FPP and heat-insulated

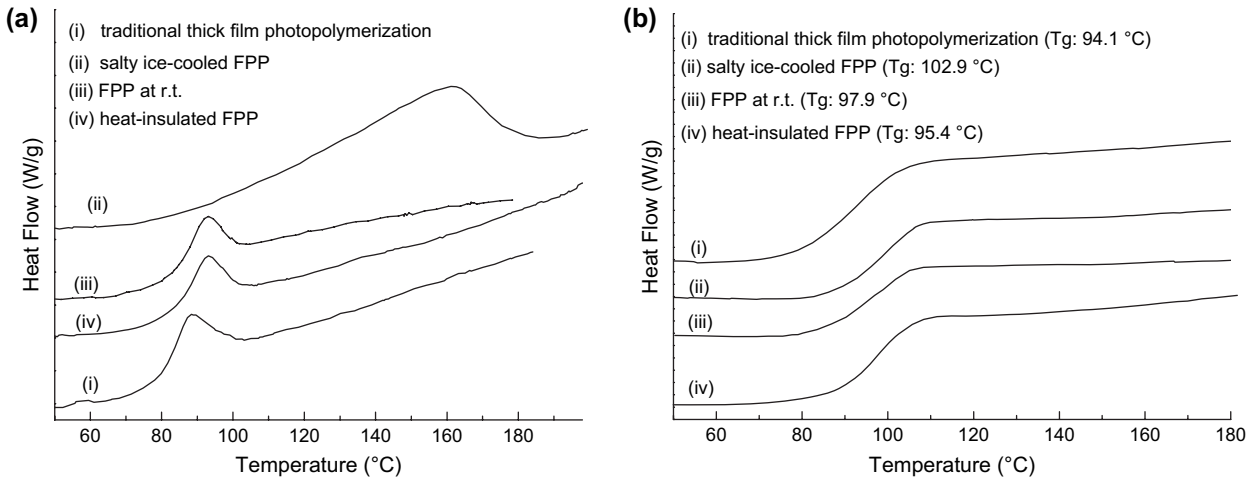

Fig. 9. DSC traces of poly(IBOA) obtained at different conditions (light intensity 5.5 mW/cm^2): (a) the first scanning and (b) the second scanning after quenching in liquid nitrogen.

FPP, the similar enthalpic peaks accounted for similar entanglement in polymer. It could be ascribed to their similar thermal experience. An unconventional great enthalpy relaxation was found for the ice-cooled FPP sample, which meant that the interacted polymer chain had to absorb more heat to disentangle. It was further implied that a lot of entanglement points were generated during the ''cold'' frontal polymerization and the free segment between two entanglement points got shorter than the aforecited three samples.

Fig. 9b, the second DSC scanning traces for the samples quenched in liquid nitrogen from 140 °C, showed that the glass transition occurred over different temperature range for the four samples. The samples produced by FPP showed rather narrow and well defined glass transitions comparing with the product of traditional thick film photopolymerization. It agreed with the results of GPC analysis in which the FPP polymers had higher molecular weight and narrower polydispersity than the thick film photopolymerization product. The oligomer present in the film photopolymerization product would have plasticization effect on the sample and broaden the glass transition. The high T_g (102.9 °C) for the ice-cooled sample might be related to the fairly narrow molecular weight distribution (depth 16–24 mm; M_w 5.47×10^5, M_n 2.57×10^5 and MWD 2.13).

4. Conclusion

An interesting oriented sleeve-like morphology was first observed in the polymer obtained *via* frontal photopolymerization at ambient temperature and heat insulation. The axisymmetric convection around the front and the sagging of the viscoelastic front were proposed to account for this unique morphology. In contrast to the traditional thick film photopolymerization, pure polymer without residual monomer was produced with the frontal photopolymerization. Lots of chain entanglements were revealed for the low temperature polymerization product. Vertical gradient distribution of the molecular weight and its polydispersity of the frontal photopolymerized rod are found, which accords with the attenuation of light intensity in the polymerization tube.

Appendix. Supplementary data

Supplementary data associated with this article can be found, in the online version, at doi:10.1016/j.polymer.2007.08.013.

References and notes

[1] Pojman JA. J Am Chem Soc 1991;113:6284.
[2] Koike Y, Hatanaka H, Otsuka Y. Appl Opt 1984;23:1779.
[3] Pojman JA, Elcan W, Khan AM, Mathias L. J Polym Sci Part A Polym Chem 1997;35:227.
[4] Washington RP, Steinbock O. J Am Chem Soc 2001;123:7933.
[5] Pojman JA, Warren J. Polym Prepr (Am Chem Soc Div Polym Chem) 1998;39:356.
[6] Righetti PG, Bossi A, Giglio M, Vailati A, Lyubimova T, Briskman VA. Electrophoresis 1994;15:1005.
[7] Cabral JT, Hudson SD, Harrison C, Douglas JF. Langmuir 2004;20:10020.
[8] Decker C, Keller L, Zahouily K, Benfarhi S. Polymer 2005;46:6640.
[9] Terrones G, Pearlstein AJ. Macromolecules 2001;34:3195.
[10] Terrones G, Pearlstein AJ. Macromolecules 2001;34:8894.
[11] Miller GA, Gou L, Narayanan V, Scranton AB. J Polym Sci Part A Polym Chem 2002;40:793.
[12] Pojman JA, Varisli B, Perryman A, Edwards C, Hoyle C. Macromolecules 2004;37:691.
[13] Decker C, Zahouily K, Decker D, Nguyen T, Viet T. Polymer 2001;42:7551.
[14] Nason C, Roper T, Hoyle C, Pojman JA. Macromolecules 2005;38:5506–12.
[15] Garbey M, Taik A, Volpert V. Preprint CNRS 1994;187:1–42.
[16] Garbey M, Taik A, Volpert V. Quart Appl Math 1998;56:1–35.
[17] Brandrup L, Immergut H, Grulkee A, editors. Polymer handbook. 4th ed., vol. VI. New York: John-Wiley and Sons; 1999. p. 200.
[18] Belk M, Kostarev KG, Volpert V, Yudina TM. J Phys Chem B 2003;107:10292.
[19] Pojman JA, Gunn G, Owens J, Simmons C. J Phys Chem B 1998;102:3927.
[20] Shaw MT, MacKnight WJ, editors. Introduction to polymer viscoelasticity. 3rd ed. Hoboken, New Jersey: John-Wiley & Sons; 2005.
[21] Pojman JA, Epstein IR. J Phys Chem 1990;94:4966.
[22] Chekanov Y, Arrington D, Brust G, Pojman JA. J Appl Polym Sci 1997;66:1209.
[23] Huang DH, Yang YM, Zhuang GQ, Li BY. Macromolecules 1999;32:6675.